



<b>Title</b>	Nanoscale Piezoelectric Properties of Self-Assembled Fmoc-FF Peptide Fibrous Networks
<b>Authors(s)</b>	Ryan, Kate, Beirne, Jason, Redmond, Gareth, Kilpatrick, J. I., Guyonnet, Jill, Buchete, Nicolae-Viorel, Kholkin, Andrei L., Rodriguez, Brian J.
<b>Publication date</b>	2015-05-21
<b>Publication information</b>	Ryan, Kate, Jason Beirne, Gareth Redmond, J. I. Kilpatrick, Jill Guyonnet, Nicolae-Viorel Buchete, Andrei L. Kholkin, and Brian J. Rodriguez. "Nanoscale Piezoelectric Properties of Self-Assembled Fmoc-FF Peptide Fibrous Networks." American Chemical Society, May 21, 2015. <a href="https://doi.org/10.1021/acsami.5b01251">https://doi.org/10.1021/acsami.5b01251</a> .
<b>Publisher</b>	American Chemical Society
<b>Item record/more information</b>	<a href="http://hdl.handle.net/10197/12003">http://hdl.handle.net/10197/12003</a>
<b>Publisher's statement</b>	This document is the Accepted Manuscript version of a Published Work that appeared in final form in ACS Applied Materials and Interfaces, copyright © 2015 American Chemical Society after peer review and technical editing by the publisher. To access the final edited and published work see <a href="http://pubs.acs.org/doi/abs/10.1021/acsami.5b01251">http://pubs.acs.org/doi/abs/10.1021/acsami.5b01251</a> .
<b>Publisher's version (DOI)</b>	10.1021/acsami.5b01251

Downloaded 2026-05-01 23:36:33

The UCD community has made this article openly available. Please share how this access benefits you. Your story matters! (@ucd\_oa)



© Some rights reserved. For more information

# Nanoscale piezoelectric properties of self-assembled Fmoc-FF peptide fibrous networks

Kate Ryan,<sup>†,‡</sup> Jason Beirne,<sup>§</sup> Gareth Redmond,<sup>§</sup> Jason Kilpatrick,<sup>‡</sup> Jill Guyonnet,<sup>†,‡</sup> Nicolae-Viorel Buchete,<sup>†,⊥</sup> Andrei L. Kholkin,<sup>||,△</sup> and Brian J. Rodriguez<sup>\*,†,‡</sup>

<sup>†</sup>School of Physics, University College Dublin, Belfield, Dublin 4, Ireland

<sup>‡</sup>Conway Institute of Biomolecular and Biomedical Research, University College Dublin, Belfield, Dublin 4, Ireland

<sup>§</sup>School of Chemistry and Chemical Biology, University College Dublin, Belfield, Dublin 4, Ireland

<sup>⊥</sup>Complex and Adaptive Systems Laboratory, University College Dublin, Belfield, Dublin 4, Ireland

<sup>||</sup>Department of Ceramics and Glass Engineering & CICECO, University of Aveiro, 3810-193 Aveiro, Portugal

<sup>△</sup>Ural Federal University, Lenin Ave. 51, Ekaterinburg 620083, Russia

**ABSTRACT:** Fibrous peptide networks, such as the structural framework of self-assembled fluorenylmethyloxycarbonyl diphenylalanine (Fmoc-FF) nanofibrils, have mechanical properties that could successfully mimic natural tissues, making them promising materials for tissue engineering scaffold materials. These nanomaterials have been determined to exhibit shear piezoelectricity using piezoresponse force microscopy, as previously reported for FF nanotubes. Structural analyses of Fmoc-FF nanofibrils suggest that the observed piezoelectric response may result from the non-centrosymmetric nature of an underlying  $\beta$ -sheet topology. The observed piezoelectricity of Fmoc-FF fibrous networks is advantageous for a range of biomedical applications where electrical or mechanical stimuli are required.

1  
2  
3 **KEYWORDS:** piezoelectricity, peptides, piezoresponse force microscopy, hydrogels,  
4  
5 biomaterials  
6  
7

## 10 1. INTRODUCTION

11 Self-assembling aromatic peptides have an intrinsic ability to form highly ordered  
12 nanostructures, i.e., nanospheres, nanotubes, nanofibrils, etc.<sup>1-4</sup> Spontaneous self-assembly  
13 occurs at the nanoscale through conformational packing and linkage between amino acid  
14 sequences.<sup>5-7</sup> The presence of aromatic interactions, non-covalent interactions (hydrogen bonds,  
15 van der Waals and electrostatics) and  $\pi$ - $\pi$  stacking stabilize the structure with superior stiffness,  
16 thermal and chemical stability possible.<sup>8,9</sup> Additionally, the biological nature of the building  
17 blocks facilitates their application to many areas such as bio-sensing, drug delivery and tissue  
18 engineering.<sup>10</sup>  
19  
20  
21  
22  
23  
24  
25  
26  
27  
28  
29  
30

31 Diphenylalanine (FF) is a common peptide occurring naturally as the core derivative of  
32 amyloid beta ( $\beta$ ) protein. It self-assembles into a number of well-characterized nanostructures,  
33 including nanotubes, through thermodynamic folding of the  $\beta$ -sheet.<sup>1,2,4,11-13</sup> The  $\beta$ -sheet  
34 conformation is the well-established structure of many peptides and proteins, most notably the  
35 structure of amyloids, a protein with many functional properties in nature<sup>14</sup> associated with  
36 numerous diseases.<sup>15,16</sup> FF nanotubes are widely regarded as useful nanomaterials, possessing  
37 good thermal, mechanical and piezoelectric properties.<sup>17,18</sup> Piezoelectricity is an inherent  
38 characteristic of non-centrosymmetric materials, whereby the material will generate electric  
39 charge under a mechanical stress or the material will undergo a mechanical deformation when  
40 subjected to an applied electric field.<sup>4</sup> The presence of electromechanical coupling in biological  
41 systems is an established phenomenon, e.g., both neurons and muscle control utilize a voltage-  
42 controlled stress or strain mechanism.<sup>19-24</sup> Using piezoresponse force microscopy (PFM),  
43  
44  
45  
46  
47  
48  
49  
50  
51  
52  
53  
54  
55  
56  
57  
58  
59  
60

1  
2  
3 Kholkin *et al.* have demonstrated that FF nanotubes are piezoelectric, exhibiting shear  
4 piezoelectricity along their longitudinal axis attributed to the non-centrosymmetric nature of the  
5  $\beta$ -sheet.<sup>17</sup>  
6  
7

8  
9  
10 A similar system consists of FF peptides modified with an added fluorenyl-methoxycarbonyl  
11 (Fmoc) side group, which self-assembles to form a three-dimensional network of ordered Fmoc-  
12 FF nanofibrils via molecular stacking, facilitated by the presence of the Fmoc moiety and  
13 mediated by non-covalent interactions.<sup>11,13,25</sup> The Fmoc-FF molecular structure has been  
14 suggested to consist of molecules in a  $\beta$ -sheet conformation with a high degree of  $\pi$ - $\pi$   
15 stacking.<sup>13,26</sup> The structural similarity of the Fmoc-FF nanofibrils to the piezoelectric FF  
16 nanotubes suggests that Fmoc-FF hydrogels may also be piezoelectric.  
17  
18  
19

20  
21  
22 In general, hydrogels are highly adaptable materials, which can be used to mimic natural tissue,  
23 support cell attachment and enhance cell differentiation and survival.<sup>27-29</sup> Fmoc-FF hydrogels  
24 have a structure and viscoelasticity comparable to that of extracellular matrices and are  
25 promising organic materials for tissue engineering applications.<sup>13,25</sup> For example, Liebmann *et*  
26 *al.* have shown that cells suspended in an Fmoc-FF hydrogel tend to adopt a three-dimensional  
27 structure that may more accurately represent cellular shapes *in vivo*, in contrast to the elongated  
28 cellular conformations observed for surface cell cultures.<sup>30</sup> The hydrogels were further shown to  
29 have improved biocompatibility for cell cultures as compared to alternative biopolymer  
30 materials.<sup>30</sup> Fmoc-FF hydrogels have also been reported to be cytotoxic upon dissolution,<sup>31</sup>  
31 highlighting the need to carefully control the parameters of such assays.  
32  
33  
34  
35  
36  
37  
38  
39  
40  
41  
42  
43  
44  
45  
46  
47  
48  
49

50  
51 In the field of tissue engineering, a scaffold possessing piezoelectric properties could be  
52 particularly useful, as bone remodeling and nerve regeneration have both been identified as being  
53 sensitive to piezoresponse. The direct piezoelectric effect has been linked with the ability of bone  
54  
55  
56  
57  
58  
59  
60

1  
2  
3 to remodel in response to an applied stress.<sup>22,32,33</sup> Piezoelectricity has also been identified as a  
4 precursor to successful axonal regeneration following nerve injury.<sup>34</sup> Therefore, a robust,  
5 biocompatible piezoelectric scaffold could provide functional tissue analogues. Here, we  
6 investigate piezoelectricity in dried Fmoc-FF peptide hydrogels using PFM.  
7  
8  
9  
10  
11

## 12 13 14 15 **2. EXPERIMENTAL SECTION**

16  
17 *2.1 Peptide preparation.* Fmoc-FF hydrogels were prepared using a solvent-based method.<sup>12,25</sup>  
18 Fmoc-FF monomer (B2150, Bachem AG) was dissolved in dimethyl sulphoxide (DMSO)  
19 (472301, Sigma Aldrich) at a concentration of 100 mg mL<sup>-1</sup>. The hydrogel was subsequently  
20 prepared by diluting the stock solution in double distilled H<sub>2</sub>O (ddH<sub>2</sub>O) to a final concentration  
21 of 5 mg mL<sup>-1</sup> (final hydrogel pH was 4–5).  
22  
23  
24  
25  
26  
27

28  
29 FF nanotubes were also prepared as a reference sample by dissolving the FF monomer (G-2925  
30 Bachem AG) in lyophilized form in 1,1,1,3,3,3-hexafluoro-2-propanol (105228, Sigma Aldrich)  
31 at a concentration of 100 mg mL<sup>-1</sup>.<sup>7</sup> The FF stock solution was diluted to a final concentration of  
32 2 mg mL<sup>-1</sup> in ddH<sub>2</sub>O for nanotube self-assembly.  
33  
34  
35  
36  
37

38  
39 *2.2 Photoluminescence (PL) Fmoc-FF solution & gel.* Fmoc-FF was dissolved in DMSO (1.1  
40 mg mL<sup>-1</sup>) in a quartz cuvette and using a silicone isolator, 500 μm-thick gel layers were prepared  
41 on fused silica (U01-120924-1, University Wafer). PL spectra were acquired using a steady state  
42 spectrofluorometer (Quantamaster 40, Photon Technology International Inc.) using a thin film  
43 holder. Acquisition settings of 1 nm step size, 0.1 s integration time, and a 300 – 900 nm scan  
44 range were used. Excitation and emission slits were set to 3 nm and 1 nm, respectively.  
45  
46  
47  
48  
49  
50  
51

52  
53 *2.3 Circular dichroism.* Circular dichroism (CD) spectra were acquired on a  
54 spectropolarimeter (J-810, Jasco Inc.). Five fused silica capillaries (5010S-050, VitroCom) were  
55 filled with gel solution, which was allowed to set. Each capillary was sealed with vacuum grease  
56  
57  
58  
59  
60

1  
2  
3 (Dow Corning) and mounted onto a glass frame, which was placed in the path of the light beam.  
4  
5 Scans were recorded from 170 nm to 350 nm, at 5 nm bandwidth and 1 s integration time. The  
6  
7 background signal was recorded from blank fused silica capillaries and subtracted to obtain each  
8  
9 CD spectrum.  
10

11  
12 *2.4 Attenuated total reflectance Fourier transform infrared (ATR-FTIR) spectroscopy.* 2 mL of  
13  
14 gel was deposited onto a zinc selenide horizontal flat plate ATR window (PIKE Technologies,  
15  
16 Inc.). The hydrogel layer was allowed to dry onto the window to minimize any water response.  
17  
18 The dried sample was then wetted three times with 2 mL of  $^2\text{H}_2\text{O}$  ( $\text{D}_2\text{O}$ ). Scans were performed  
19  
20 on a FTIR spectrometer (Cary 680, Agilent Technologies, Inc.) at a resolution of  $4\text{ cm}^{-1}$  over 64  
21  
22 accumulations. The background signal was recorded from zinc selenide with  $\text{D}_2\text{O}$  and subtracted  
23  
24 to obtain each FTIR spectrum.  
25  
26

27  
28 *2.5 Atomic force microscopy and PFM.* Contact mode atomic force microscopy (AFM) and  
29  
30 PFM measurements (MFP-3D, Asylum Research) were performed using Pt-coated Si cantilevers  
31  
32 (MikroMasch CSC37 lever A, HQ:DPE-XSC11 lever B and HQ:DPE-XSC11 lever C with  
33  
34 nominal resonant frequencies of 30 kHz, 80 kHz, and 155 kHz and nominal spring constants of  
35  
36  $0.8\text{ N m}^{-1}$ ,  $2.7\text{ N m}^{-1}$  and  $7\text{ N m}^{-1}$ , respectively). A lock-in amplifier (HF2LI, Zurich Instruments)  
37  
38 and a high voltage power supply (F10A, FLC Electronics AB) were employed to enable PFM.  
39  
40 The cantilevers were calibrated using the thermal noise method and force spectroscopy to  
41  
42 establish the spring constant and deflection inverse optical lever sensitivity.<sup>35</sup> The lateral inverse  
43  
44 optical lever sensitivity was determined following Peter *et al.*<sup>36</sup> and taking into account the gain  
45  
46 ratio between the deflection and lateral signals (measured to be 4.0 for the AFM used).  
47  
48 Uncertainty was estimated as 10% for the deflection inverse optical lever sensitivity, which was  
49  
50 then used to calculate errors for all derived values.  
51  
52  
53  
54  
55  
56  
57  
58  
59  
60

1  
2  
3 Prior to measurements, 20  $\mu\text{L}$  of the samples were deposited on as-received glass slides (631-  
4 0907, VWR) and dried under ambient conditions (21  $^{\circ}\text{C}$ , humidity  $\sim 30\%$ ) for 24 hours, with  
5 evaporation aiding the process of self-assembly in the case of the FF nanotubes. An AC voltage  
6 was applied to the samples via a conductive tip scanned in contact with the surface with a typical  
7 loading force of  $\sim 12$  nN and a typical scan rate of  $\sim 0.3$  Hz. Lateral PFM (LPFM) was  
8 performed using an imaging voltage of 30  $V_{\text{rms}}$  applied at a frequency of 5 kHz (to FF sample)  
9 and 12.5 kHz (to Fmoc-FF sample). The lock-in amplifier demodulated the cantilever response  
10 due to sample deformations into amplitude and phase piezoresponse signals. A 3 ms time  
11 constant was used throughout. For measurements of the piezoelectric coefficient,<sup>37</sup> the tip was  
12 placed in contact with the surface of both samples with a loading force of 10 nN at specific  
13 locations and a 5 kHz (FF sample) and 12.5 kHz (Fmoc-FF sample) AC voltage was swept from  
14 0 to 60  $V_{\text{rms}}$  in 6  $V_{\text{rms}}$  increments whilst recording LPFM response.  
15  
16  
17  
18  
19  
20  
21  
22  
23  
24  
25  
26  
27  
28  
29  
30  
31  
32  
33

### 34 **3. RESULTS AND DISCUSSION**

35  
36 *3.1. Structural Characterization.* PL spectra allowed monitoring of the environment of the Fmoc  
37 moiety to assess the role of intermolecular interactions during peptide aggregation. The solution  
38 emission spectrum of Fmoc-FF (i.e., Fmoc-FF/DMSO) had a peak with a maximum intensity at  
39 313 nm; see Figure 1. By comparison, the emission spectrum of a gel sample (Fmoc-  
40 FF/Hydrogel) showed an intensity maximum at 324 nm.  
41  
42  
43  
44  
45  
46  
47  
48  
49  
50  
51  
52  
53  
54  
55  
56  
57  
58  
59  
60

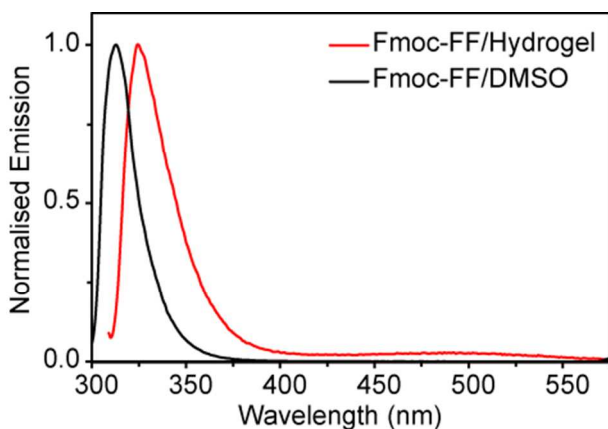


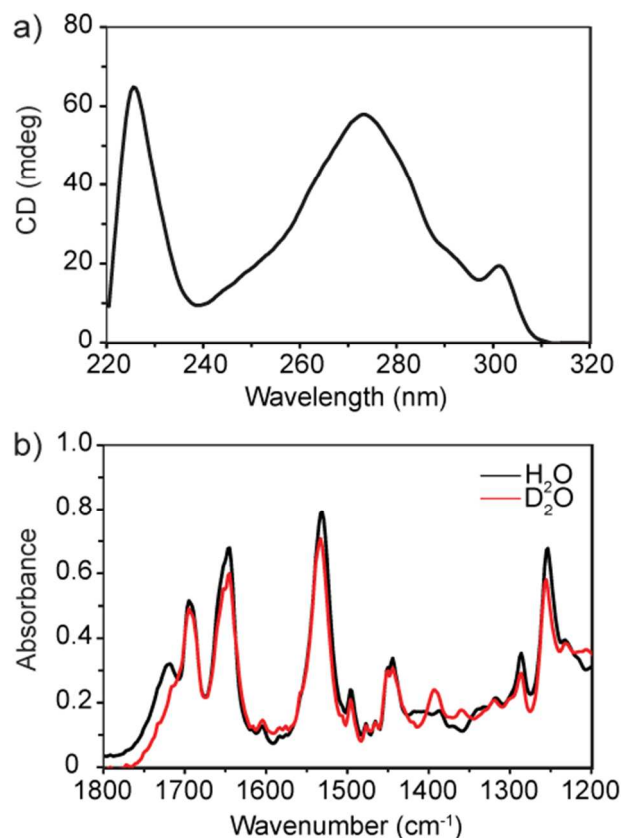
**Figure 1.** Fluorescence emission spectra measured for Fmoc-FF in solvent and hydrogel phases.

This red-shift of the emission maximum from 313 to 324 nm was likely due to an increase in the dielectric constant of the environment around each fluorenyl chromophore and a transition from free molecules in the solution phase to a more aggregated and organized molecular structure in the gel phase. For example, fluorenyl aggregation could occur via  $\pi$ - $\pi$  stacking interactions, possibly with an anti-parallel arrangement of the fluorenyl moieties.<sup>13,38</sup> Additionally, the gel PL emission spectrum also exhibited a broad feature with a maximum near 500 nm, likely due to emission from fluorenyl excimer species.<sup>39</sup>

To obtain further insight into the nature of the aggregated state in the gel phase, CD spectroscopy was applied to the Fmoc-FF hydrogels (gelation in ddH<sub>2</sub>O); see Figure 2a. A Cotton effect at 226 nm ( $n\pi^*$  transition) indicated a super-helical arrangement of the phenylalanine residues, which induced a helical orientation of the fluorenyl moieties (the Cotton effect at 273–301 nm,  $\pi\pi^*$  transitions) in the hydrogel.<sup>38,40-42</sup>

More detailed information regarding the arrangement of the Fmoc-FF residues with the hydrogel samples was obtained by acquiring FTIR spectra of hydrogels (gelation in ddH<sub>2</sub>O followed by drying and subsequent treatment with D<sub>2</sub>O) in attenuated total reflectance mode; see Figure 2b. The resulting spectra exhibited distinct spectral bands at 1695 cm<sup>-1</sup>, 1645 cm<sup>-1</sup>, 1533

1  
2  
3  $\text{cm}^{-1}$ , and  $1255 \text{ cm}^{-1}$ . While the feature at  $1695 \text{ cm}^{-1}$  has in the past been associated with  $\beta$ -turn or  
4 anti-parallel  $\beta$ -sheet conformations, it has recently also been attributed to carbamate  
5 absorption.<sup>43-46</sup> Also in the amide I region, the peak at  $1645 \text{ cm}^{-1}$  has previously been reported  
6 for materials containing  $\beta$ -sheet, alpha ( $\alpha$ )-helical or random coil peptide arrangements, and, in  
7 the amide II and amide III regions, peaks at  $1533 \text{ cm}^{-1}$  and at  $1255 \text{ cm}^{-1}$ , respectively, have been  
8 associated with either a  $\beta$ -turn or an anti-parallel  $\beta$ -sheet secondary structure.<sup>44</sup>  
9  
10  
11  
12  
13  
14  
15  
16  
17



46 **Figure 2.** (a) CD spectrum of Fmoc-FF hydrogel and (b) ATR-FTIR spectra of Fmoc-FF  
47 hydrogel and Fmoc-FF hydrogel prepared with  $\text{D}_2\text{O}$ .  
48  
49

50  
51  
52 **3.2. AFM.** The topography of the samples was characterized by contact mode AFM.  
53 Topography images of FF nanotubes and dried Fmoc-FF hydrogels are shown in Figure 3a,d.  
54 The nanotubes are known to have a wide range of diameters from 100 nm up to several  
55  
56  
57  
58  
59  
60

1  
2  
3 microns.<sup>7,47</sup> The average diameter of the nanotubes in this sample, as determined from their  
4  
5 height (Figure 3a), was  $667 \pm 170$  nm ( $n = 10$ ). The nanofibrils within the dense, layered Fmoc-  
6  
7 FF matrix had an average diameter of  $66 \pm 4$  nm ( $n = 21$ ) (Figure 3d).  
8  
9

10  
11 3.3. PFM. To characterize the piezoresponse of both samples, PFM was used. This method  
12  
13 involves a modified AFM, whereby an electric voltage is applied to the surface via a conducting  
14  
15 tip. Using LPFM piezoelectric deformations can be measured via the torsion of the cantilever. In  
16  
17 the case of an FF nanotube lying flat on a substrate, LPFM therefore allows shear deformation to  
18  
19 be measured. Previously, Kholkin *et al.* reported robust LPFM signals, with an expected  
20  
21 dependence on the angle between the cantilever and the FF nanotube, for this configuration.<sup>17</sup>  
22  
23

24  
25 Using LPFM, a piezoelectric response was found in self-assembled FF nanotubes in agreement  
26  
27 with literature.<sup>17</sup> The LPFM amplitude and phase images of the FF nanotubes are shown in  
28  
29 Figure 3b and 3c, respectively. The LPFM amplitude signal is maximal when the cantilever and  
30  
31 nanotube longitudinal axes are orthogonal, such as the nanotube marked by an arrow in Fig. 3b.  
32  
33 In the LPFM phase image, nanotubes having opposite polarization directions can be identified  
34  
35 (the piezoresponse of purple and yellow nanotubes in Figure 3c have a  $180^\circ$  phase shift).  
36  
37

38  
39 The LPFM amplitude and phase images for the dried Fmoc-FF hydrogel are shown in Figure 3e  
40  
41 and 3f, respectively. The Fmoc-FF nanofibrils within the gel exhibited an apparent shear  
42  
43 response, however, strong angle dependency of the LPFM amplitude of the nanofibers was not  
44  
45 observed, possibly due to the complex arrangement of the nanofibrils and resolution limits of the  
46  
47 technique. In some cases, the phase signal inverts along the length of a fibril, highlighting the  
48  
49 heterogeneous nature of the nanofibril network.  
50  
51

52  
53 As PFM images can contain a background offset signal, in order to quantify the piezoresponse  
54  
55 of the FF nanotubes and the Fmoc-FF nanofibrils, the LPFM amplitude was measured as a  
56  
57  
58  
59  
60

1  
2  
3 function of applied voltage (Figure 4). The LPFM signal was observed to be linearly dependent  
4  
5 on the applied voltage within experimental error. This method provides a value for the  $d_{35}$   
6  
7 component of the piezoelectric tensor in the laboratory coordinate system,<sup>48</sup> the measured in-  
8  
9 plane effective piezoelectric coefficient obtained from the slope. All measurements carried out  
10  
11 on nanotubes and nanofibrils assume that the sample response is orthogonal to the cantilever in  
12  
13 the  $X$ - $Y$  plane. Under this assumption, it is possible to directly determine the  $d_{15}$  component of  
14  
15 the piezoelectric tensor of a shear piezoelectric sample (hereafter called  $d_{15}^0$ , where the  
16  
17 superscript denotes that the coefficient belongs to the sample coordinate system). The  $d_{15}^0$  for the  
18  
19 nanotubes was determined to be  $33.7 \pm 0.7 \text{ pm V}^{-1}$  ( $n = 5$ ) and for the nanofibrils,  $d_{15}^0$  was  
20  
21 determined to be  $1.7 \pm 0.5 \text{ pm V}^{-1}$  ( $n = 5$ ). The latter is significantly greater than the system  
22  
23 detection limits as estimated by measuring  $d_{35}$  on non-piezoelectric glass, which was determined  
24  
25 to be  $0.002 \pm 0.103 \text{ pm V}^{-1}$  ( $n = 5$ ).  
26  
27  
28  
29  
30  
31  
32  
33  
34  
35  
36  
37  
38  
39  
40  
41  
42  
43  
44  
45  
46  
47  
48  
49  
50  
51  
52  
53  
54  
55  
56  
57  
58  
59  
60

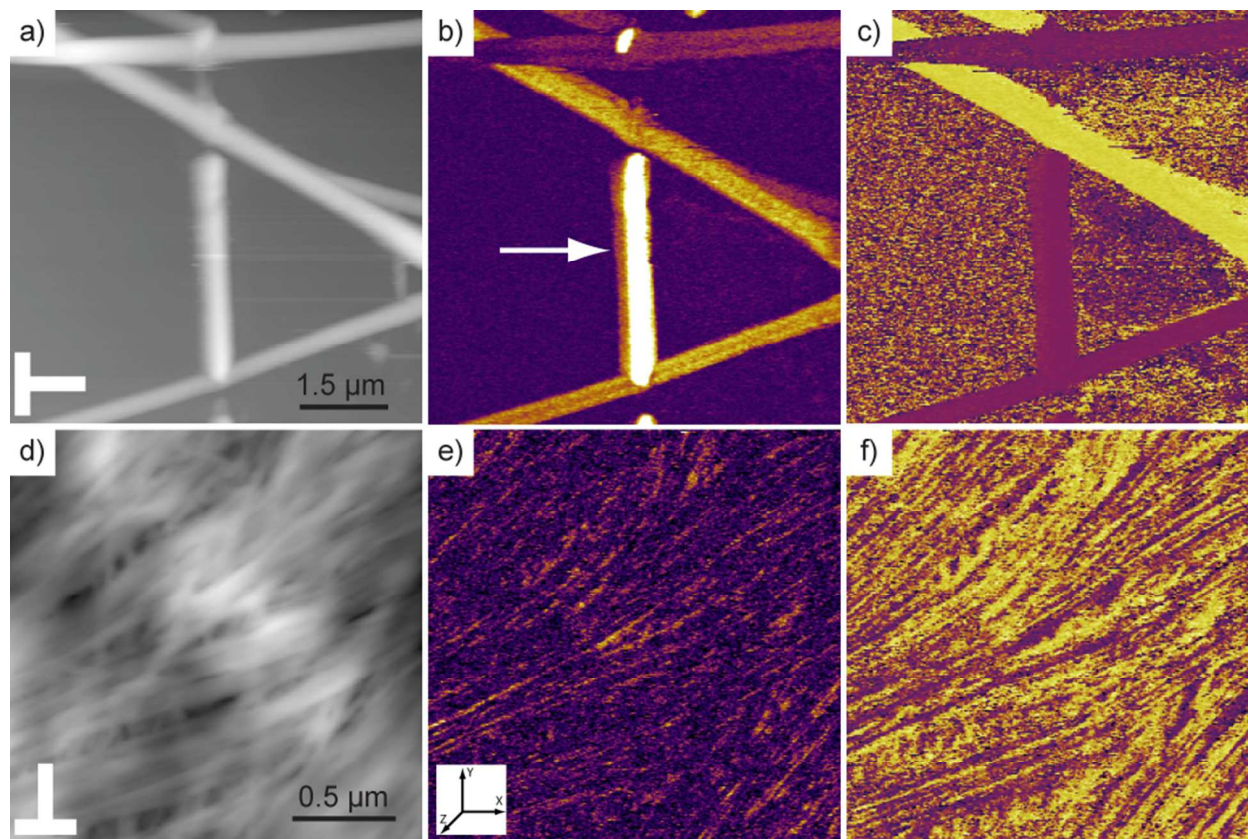


**Figure 3.** (a, d) AFM topography and LPFM (b, e) amplitude and (c, f) phase images of FF nanotubes and Fmoc-FF nanofibrils, respectively. The Z-scale data ranges are 400 nm and 80 nm for (a) and (d), 200 pm and 80 pm for (b) and (e) with both images offset by 150 pm, and 180° for (c) and (f). The arrow in (b) indicates an FF nanotube orthogonal to cantilever axis. The inset in (e) shows the laboratory coordinate system.

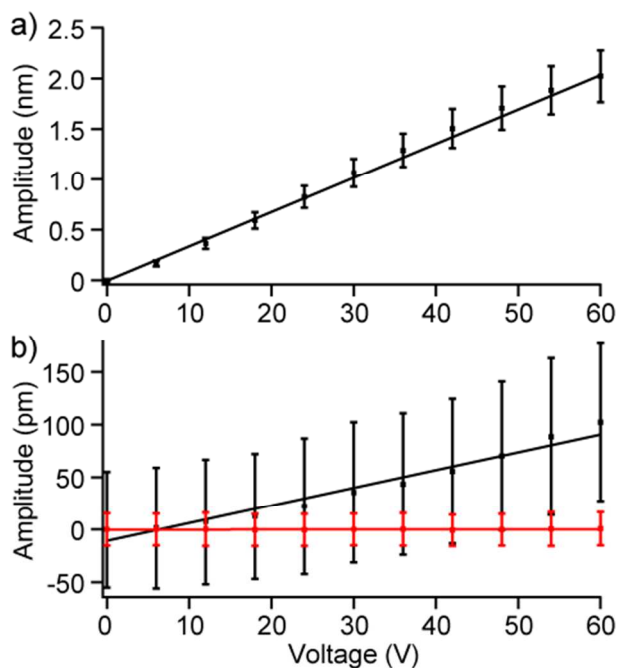


**Figure 4.** LPFM amplitude versus applied voltage (RMS) recorded on (a) FF nanotubes and (b) Fmoc-FF nanofibrils (black). The slopes provide the average local piezoelectric coefficient,  $d_{15}^0$ , for nanotubes and nanofibrils with an assumed orientation orthogonal to the cantilever. For comparison, the piezoresponse signal measured for a non-piezoelectric glass slide (red) is shown in (b).

**3.4. Discussion.** The source of piezoelectricity in amyloid fibrils and FF nanotubes is attributed to the collective dipole, or polarization, present due to the arrangement of  $\beta$ -sheets.<sup>23,49,50</sup> Recent atomistic molecular dynamics simulations of FF peptides have shown that individual molecular dipoles depend on the detailed charge state of peptide termini, on the molecular backbone conformational dynamics, as well as on the magnitude of local electric fields.<sup>4</sup> The self-assembly propensity of FF peptides in nanomaterials and their piezoelectric properties are therefore interdependent.<sup>4</sup> Anti-parallel  $\beta$ -sheets present dipoles perpendicular to the direction of the  $\beta$ -strands, creating an overall polarization along the fibril/nanotube axis.<sup>51</sup> Mahler *et al.* have shown that the

1  
2  
3 structure of the Fmoc-FF nanofibrils is consistent with the  $\beta$ -sheet and  $\beta$ -turn conformation  
4 present in amyloid fibrils and FF nanotubes.<sup>52</sup> Smith *et al.* have previously proposed a model  
5 structure for the Fmoc-FF nanofibrils, formed from antiparallel  $\beta$ -sheets, whereby the natural  
6 twist in the  $\beta$ -sheet leads to the combination of four sheets, creating a cylindrical nanofibril with  
7 a typical diameter of  $\sim 3$  nm.<sup>13</sup> The available evidence for Fmoc-FF secondary structure indicates  
8 that the  $\beta$ -sheet is rolled in a similar fashion with each  $\beta$ -strand perpendicular to the fibril axis,  
9 which suggests a net polarization along the fibril axis could be possible.<sup>51</sup> The nanofibrils  
10 observed in this study have an average diameter of  $66 \pm 4$  nm, suggesting the predicted  $\sim 3$  nm  
11 nanofibrils are in bundles, as has been previously observed for similar materials, e.g., peptide-  
12 amphiphiles.<sup>28</sup> These results highlight the ability of potentially biocompatible peptides to form  
13 piezoelectrically-active structures, which may lead to possible bio-applications.  
14  
15  
16  
17  
18  
19  
20  
21  
22  
23  
24  
25  
26  
27  
28  
29  
30

#### 31 **4. SUMMARY**

32 Fibrous peptide networks composed of self-assembled Fmoc-FF nanofibrils were shown to  
33 exhibit shear piezoelectricity by measuring their characteristic local in-plane piezoelectric  
34 response using LPFM. Structural characterization suggested that Fmoc-FF nanofibrils present a  
35 non-centrosymmetric  $\beta$ -sheet structure, consistent with the mechanism reported for piezoelectric  
36 FF nanotubes.<sup>17</sup> Since peptide hydrogels are bio-mimetic materials with mechanical properties  
37 comparable to those of biological gels, the added functionality arising from their piezoelectricity  
38 could enable the application of these hydrogels in developing novel piezoelectric scaffolds for  
39 tissue engineering.  
40  
41  
42  
43  
44  
45  
46  
47  
48  
49  
50  
51  
52  
53  
54

#### 55 **AUTHOR INFORMATION**

##### 56 **Corresponding Author**

57  
58  
59  
60

1  
2  
3 \*E-mail: brian.rodriquez@ucd.ie  
4  
5

### 6 **Author Contributions**

7  
8 The manuscript was written through contributions of all authors. All authors have given approval  
9  
10 to the final version of the manuscript.  
11

### 12 **Notes**

13  
14 The authors declare no competing financial interest.  
15  
16

### 17 **ACKNOWLEDGMENT**

18  
19 The work is supported by the European Commission within FP7 Marie Curie Initial Training  
20  
21 Network "Nanomotion" (grant agreement n° 290158). Additional financial support was provided  
22  
23 by NANOREMEDIES, which is funded under Cycle 5 of the Programme for Research in Third  
24  
25 Level Institutions and co-funded by the European Regional Development Fund. The authors  
26  
27 gratefully acknowledge Tim Brosnan for AFM transfer function characterization and Dr. B.  
28  
29 Lukasz for assistance with scanning electron microscopy of the cantilevers used. The AFM used  
30  
31 for this work was funded by Science Foundation Ireland (SFI07/IN1/B931).  
32  
33  
34

35  
36 **ABREVIATIONS:** Fluorenylmethyloxycarbonyl diphenylalanine (Fmoc-FF), diphenylalanine  
37  
38 (FF), piezoresponse force microscopy (PFM), double distilled H<sub>2</sub>O (ddH<sub>2</sub>O), dimethyl  
39  
40 sulphoxide (DMSO), photoluminescence (PL), circular dichroism (CD), lateral PFM (LPFM)  
41  
42  
43  
44

### 45 **REFERENCES**

- 46  
47 (1) Görbitz, C. H. Nanotube Formation by Hydrophobic Dipeptides. *Chem. Eur. J.* **2001**, *7*,  
48  
49 5153-5159.  
50  
51  
52 (2) Gazit, E. Self-Assembled Peptide Nanostructures: The Design of Molecular Building  
53  
54 Blocks and Their Technological Utilization. *Chem. Soc. Rev.* **2007**, *36*, 1263-1269.  
55  
56  
57  
58  
59  
60

- 1  
2  
3 (3) Görbitz, C. H. Structures of Dipeptides: The Head-to-Tail Story. *Acta Crystallogr., Sect.*  
4 *B: Struct. Sci.* **2010**, *66*, 84-93.  
5  
6  
7  
8 (4) Kelly, C. M.; Northey, T.; Ryan, K.; Brooks, B. R.; Kholkin, A. L.; Rodriguez, B. J.;  
9 Buchete, N.-V. Conformational Dynamics and Aggregation Behavior of Piezoelectric  
10 Diphenylalanine Peptides in an External Electric Field. *Biophys. Chem.* **2015**, *196*, 16-24.  
11  
12  
13 (5) Ghadiri, M. R.; Granja, J. R.; Milligan, R. A.; McRee, D. E.; Khazanovich, N. Self-  
14 Assembling Organic Nanotubes Based on a Cyclic Peptide Architecture. *Nature* **1993**,  
15 *366*, 324-327.  
16  
17  
18 (6) Gazit, E. ChemInform Abstract: The “Correctly Folded” State of Proteins: Is it a  
19 Metastable State? *Angew. Chem. Int. Ed.* **2002**, *33*, 257-259.  
20  
21  
22 (7) Reches, M.; Gazit, E. Casting Metal Nanowires Within Discrete Self-Assembled Peptide  
23 Nanotubes. *Science* **2003**, *300*, 625-627.  
24  
25  
26 (8) Adler-Abramovich, L.; Kol, N.; Yanai, I.; Barlam, D.; Shneck, R. Z.; Gazit, E.; Rousso,  
27 I. Self-Assembled Organic Nanostructures with Metallic-Like Stiffness. *Angew. Chem.*  
28 **2010**, *122*, 10135-10138.  
29  
30  
31 (9) Kol, N.; Adler-Abramovich, L.; Barlam, D.; Shneck, R. Z.; Gazit, E.; Rousso, I. Self-  
32 Assembled Peptide Nanotubes Are Uniquely Rigid Bioinspired Supramolecular  
33 Structures. *Nano Lett.* **2005**, *5*, 1343-1346.  
34  
35  
36 (10) Gao, X.; Matsui, H. Peptide-Based Nanotubes and Their Applications in  
37 Bionanotechnology. *Adv. Mater.* **2005**, *17*, 2037-2050.  
38  
39  
40 (11) Reches, M.; Gazit, E. Self-Assembly of Peptide Nanotubes and Amyloid-Like Structures  
41 by Charged-Termini-Capped Diphenylalanine Peptide Analogues. *Isr. J. Chem.* **2005**, *45*,  
42 363-371.  
43  
44  
45  
46  
47  
48  
49  
50  
51  
52  
53  
54  
55  
56  
57  
58  
59  
60

- 1  
2  
3  
4  
5  
6  
7  
8  
9  
10  
11  
12  
13  
14  
15  
16  
17  
18  
19  
20  
21  
22  
23  
24  
25  
26  
27  
28  
29  
30  
31  
32  
33  
34  
35  
36  
37  
38  
39  
40  
41  
42  
43  
44  
45  
46  
47  
48  
49  
50  
51  
52  
53  
54  
55  
56  
57  
58  
59  
60
- (12) Orbach, R.; Adler-Abramovich, L.; Zigerson, S.; Mironi-Harpaz, I.; Seliktar, D.; Gazit, E. Self-Assembled Fmoc-Peptides as a Platform for the Formation of Nanostructures and Hydrogels. *Biomacromolecules* **2009**, *10*, 2646-2651.
- (13) Smith, A. M.; Williams, R. J.; Tang, C.; Coppo, P.; Collins, R. F.; Turner, M. L.; Saiani, A.; Ulijn, R. V. Fmoc-Diphenylalanine Self Assembles to a Hydrogel via a Novel Architecture Based on  $\pi$ - $\pi$  Interlocked  $\beta$ -Sheets. *Adv. Mater.* **2008**, *20*, 37-41.
- (14) Jarvis, S.; Mostaert, A.: *The Functional Fold: Amyloid Structures in Nature*; CRC Press, 2012.
- (15) Gazit, E. Mechanisms of Amyloid Fibril Self-Assembly and Inhibition. *FEBS J.* **2005**, *272*, 5971-5978.
- (16) Cherny, I.; Gazit, E. Amyloids: Not Only Pathological Agents but Also Ordered Nanomaterials. *Angew Chem. Int. Ed.* **2008**, *47*, 4062-4069.
- (17) Kholkin, A.; Amdursky, N.; Bdikin, I.; Gazit, E.; Rosenman, G. Strong Piezoelectricity in Bioinspired Peptide Nanotubes. *ACS Nano* **2010**, *4*, 610-614.
- (18) Adler-Abramovich, L.; Reches, M.; Sedman, V. L.; Allen, S.; Tendler, S. J. B.; Gazit, E. Thermal and Chemical Stability of Diphenylalanine Peptide Nanotubes: Implications for Nanotechnological Applications. *Langmuir* **2006**, *22*, 1313-1320.
- (19) Shamos, M. H. Piezoelectric Effect in Bone. *Nature* **1963**, *197*, 81.
- (20) Horiuchi, S.; Tokura, Y. Organic Ferroelectrics. *Nat. Mater.* **2008**, *7*, 357-366.
- (21) Zilberstein, R. M. Piezoelectric Activity in Invertebrate Exoskeletons. *Nature* **1972**, *235*, 174-175.
- (22) Fukada, E., Yasuda, I., On the Piezoelectricity of Bone. *J. Phys. Soc. Jpn.* **1957**, *12*, 1158-1162.

- 1  
2  
3  
4  
5  
6  
7  
8  
9  
10  
11  
12  
13  
14  
15  
16  
17  
18  
19  
20  
21  
22  
23  
24  
25  
26  
27  
28  
29  
30  
31  
32  
33  
34  
35  
36  
37  
38  
39  
40  
41  
42  
43  
44  
45  
46  
47  
48  
49  
50  
51  
52  
53  
54  
55  
56  
57  
58  
59  
60
- (23) Kalinin, S. V.; Rodriguez, B. J.; Jesse, S.; Seal, K.; Proksch, R.; Hohlbauch, S.; Revenko, I.; Thompson, G. L.; Vertegel, A. A. Towards Local Electromechanical Probing of Cellular and Biomolecular Systems in a Liquid Environment. *Nanotechnology* **2007**, *18*, 424020.
- (24) Kalinin, S. V.; Rodriguez, B. J.; Jesse, S.; Thundat, T.; Gruverman, A. Electromechanical Imaging of Biological Systems with Sub-10 nm Resolution. *Appl. Phys. Lett.* **2005**, *87*, 3901.
- (25) Orbach, R.; Mironi-Harpaz, I.; Adler-Abramovich, L.; Mossou, E.; Mitchell, E. P.; Forsyth, V. T.; Gazit, E.; Seliktar, D. The Rheological and Structural Properties of Fmoc-Peptide-Based Hydrogels: The Effect of Aromatic Molecular Architecture on Self-Assembly and Physical Characteristics. *Langmuir* **2012**, *28*, 2015-2022.
- (26) Ulijn, R. V.; Smith, A. M. Designing Peptide Based Nanomaterials. *Chem. Soc. Rev.* **2008**, *37*, 664-675.
- (27) McDonald, T.; Patrick, A.; Williams, R.; Cousins, B. G.; Ulijn, R. V.: Bio-Responsive Hydrogels for Biomedical Applications. In *Biomedical Applications of Electroactive Polymer Actuators*; John Wiley & Sons, Ltd, Chichester, UK, 2009; pp 43-59.
- (28) Smith, L. A.; Ma, P. X. Nano-Fibrous Scaffolds for Tissue Engineering. *Colloids Surf. B* **2004**, *39*, 125-131.
- (29) Smith, L. A.; Liu, X.; Ma, P. X. Tissue Engineering with Nano-Fibrous Scaffolds. *Soft Matter* **2008**, *4*, 2144-2149.
- (30) Liebmann, T.; Rydholm, S.; Akpe, V.; Brismar, H. Self-Assembling Fmoc Dipeptide Hydrogel for In Situ 3D Cell Culturing. *BMC Biotechnol.* **2007**, *7*, 88.

- 1  
2  
3  
4  
5  
6  
7  
8  
9  
10  
11  
12  
13  
14  
15  
16  
17  
18  
19  
20  
21  
22  
23  
24  
25  
26  
27  
28  
29  
30  
31  
32  
33  
34  
35  
36  
37  
38  
39  
40  
41  
42  
43  
44  
45  
46  
47  
48  
49  
50  
51  
52  
53  
54  
55  
56  
57  
58  
59  
60
- (31) Truong, W. T.; Su, Y.; Gloria, D.; Braet, F.; Thordarson, P. Dissolution and Degradation of Fmoc-Diphenylalanine Self-Assembled Gels Results in Necrosis at High Concentrations In Vitro. *Biomater. Sci.* **2015**, *3*, 298-307.
- (32) Fukada, E. History and Recent Progress in Piezoelectric Polymers. *IEEE Trans. Ultrason., Ferroelect., Freq. Control* **2000**, *47*, 1277-1290.
- (33) Denning, D.; Paukshto, M.; Habelitz, S.; Rodriguez, B. J. Piezoelectric Properties of Aligned Collagen Membranes. *J. Biomed. Mater. Res., Part B* **2014**, *102*, 284-292.
- (34) Fine, E. G.; Valentini, R. F.; Bellamkonda, R.; Aebischer, P. Improved Nerve Regeneration through Piezoelectric Vinylidene fluoride-Trifluoroethylene Copolymer Guidance Channels. *Biomaterials* **1991**, *12*, 775-780.
- (35) Hutter, J. L.; Bechhoefer, J. Calibration of Atomic-Force Microscope Tips. *Rev. Sci. Instrum.* **1993**, *64*, 1868-1873.
- (36) Peter, F.; Rudiger, A.; Szot, K.; Waser, R.; Reichenberg, B. Sample-Tip Interaction of Piezoresponse Force Microscopy in Ferroelectric Nanostructures. *IEEE Trans. Ultrason., Ferroelect., Freq. Control* **2006**, *53*, 2253-2260.
- (37) Minary-Jolandan, M.; Yu, M.-F. Nanoscale Characterization of Isolated Individual Type I Collagen Fibrils: Polarization and Piezoelectricity. *Nanotechnology* **2009**, *20*, 5706.
- (38) Zhang, Y.; Gu, H.; Yang, Z.; Xu, B. Supramolecular Hydrogels Respond to Ligand-Receptor Interaction. *J. Am. Chem. Soc.* **2003**, *125*, 13680-13681.
- (39) Schweitzer, D.; Hausser, K. H.; Haenel, M. Transannular Interaction in [2.2]Phanes:[2.2](4, 4') Diphenylphane and [2.2](2, 7) Fluorenophane. *Chem. Phys.* **1978**, *29*, 181-185.

- 1  
2  
3 (40) Yang, Z.; Gu, H.; Fu, D.; Gao, P.; Lam, J. K.; Xu, B. Enzymatic Formation of  
4 Supramolecular Hydrogels. *Adv. Mater.* **2004**, *16*, 1440-1444.  
5  
6  
7  
8 (41) Yang, Z.; Gu, H.; Zhang, Y.; Wang, L.; Xu, B. Small Molecule Hydrogels Based on a  
9 Class of Antiinflammatory Agents. *Chem. Comm.* **2004**, 208-209.  
10  
11  
12 (42) Berova, N.; Nakanishi, K.; Woody, R. W.: *Circular Dichroism: Principles and*  
13 *Applications*; Wiley-VCH New York, 2000; Vol. 912.  
14  
15  
16  
17 (43) Surewicz, W. K.; Mantsch, H. H.; Chapman, D. Determination of Protein Secondary  
18 Structure by Fourier Transform Infrared Spectroscopy: A Critical Assessment.  
19 *Biochemistry* **1993**, *32*, 389-394.  
20  
21  
22  
23  
24 (44) Krimm, S. Vibrational Spectroscopy and Conformation of Peptides, Polypeptides, and  
25 Proteins. *Adv. Protein Chem.* **1986**, *38*, 181.  
26  
27  
28  
29 (45) Fleming S.; Frederix, P. W. J. M.; Sasselli, I. R.; Hunt, N. T.; Ulijn, R. V.; Tuttle, T.  
30 Assessing the Utility of Infrared Spectroscopy as a Structural Diagnostic Tool for  $\beta$ -  
31 Sheets in Self-Assembling Aromatic Peptide Amphiphiles. *Langmuir* **2013**, *29*, 9510-  
32 9515.  
33  
34  
35  
36  
37  
38 (46) Eckes, K. M.; Mu, X.; Ruehle, M. A.; Ren, P.; Suggs, L. J.  $\beta$  Sheets Not Required:  
39 Combined Experimental and Computational Studies of Self-Assembly and Gelation of  
40 the Ester-Containing Analogue of an Fmoc-Dipeptide Hydrogelator. *Langmuir* **2014**, *30*,  
41 5287-5296.  
42  
43  
44  
45  
46  
47 (47) Rosenman, G.; Beker, P.; Koren, I.; Yevnin, M.; Bank-Srouer, B.; Mishina, E.; Semin, S.  
48 Bioinspired Peptide Nanotubes: Deposition Technology, Basic Physics and  
49 Nanotechnology Applications. *J. Pept. Sci.* **2011**, *17*, 75-87.  
50  
51  
52  
53  
54  
55  
56  
57  
58  
59  
60

- 1  
2  
3  
4  
5  
6  
7  
8  
9  
10  
11  
12  
13  
14  
15  
16  
17  
18  
19  
20  
21  
22  
23  
24  
25  
26  
27  
28  
29  
30  
31  
32  
33  
34  
35  
36  
37  
38  
39  
40  
41  
42  
43  
44  
45  
46  
47  
48  
49  
50  
51  
52  
53  
54  
55  
56  
57  
58  
59  
60
- (48) Kalinin, S. V.; Rodriguez, B. J.; Jesse, S.; Shin, J.; Baddorf, A. P.; Gupta, P.; Jain, H.; Williams, D. B.; Gruverman, A. Vector Piezoresponse Force Microscopy. *Microsc. Microanal.* **2006**, *12*, 206-220.
- (49) Nikiforov, M.; Thompson, G.; Reukov, V. V.; Jesse, S.; Guo, S.; Rodriguez, B.; Seal, K.; Vertegel, A.; Kalinin, S. V. Double-Layer Mediated Electromechanical Response of Amyloid Fibrils in Liquid Environment. *ACS Nano* **2010**, *4*, 689-698.
- (50) Heredia, A.; Bdikin, I.; Kopyl, S.; Mishina, E.; Semin, S.; Sigov, A.; German, K.; Bystrov, V.; Gracio, J.; Kholkin, A. Temperature-Driven Phase Transformation in Self-Assembled Diphenylalanine Peptide Nanotubes. *J. Phys. D: Appl. Phys.* **2010**, *43*, 462001.
- (51) Demirdöven, N.; Cheatum, C. M.; Chung, H. S.; Khalil, M.; Knoester, J.; Tokmakoff, A. Two-Dimensional Infrared Spectroscopy of Antiparallel  $\beta$ -Sheet Secondary Structure. *J. Am. Chem. Soc.* **2004**, *126*, 7981-7990.
- (52) Mahler, A.; Reches, M.; Rechter, M.; Cohen, S.; Gazit, E. Rigid, Self-Assembled Hydrogel Composed of a Modified Aromatic Dipeptide. *Adv. Mater.* **2006**, *18*, 1365-1370.

TOC/Abstract Figure

